

Annual and Semiannual variation in the ionospheric F2-layer Electron density over the Indian zone

ABSTRACT

In situ measurement carried out by the Retarding potential Analyzer (RPA) on board SROSS C2 and ROCSAT during 1995 to 2003 covering ascending and descending periods of solar cycle 23 over Indian equatorial and low latitude were used to study the annual and semiannual variation of electron density at the topside F region. The analysis has been carried out for the geomagnetic equator and $\pm 10^\circ$ magnetic latitudes. Observations reveal the existence of an equatorial asymmetry during daytime (10:00 – 14:00 hrs) with higher electron density in spring than in autumn for both ascending and descending leg of the solar cycle. At the peak of the solar cycle, the density becomes equal for both equinoxes. Nighttime (22:00 – 00:00 hrs) density in autumn is higher than that in spring for the ascending half of the solar cycle, becomes equal for both the equinoxes around the peak of the solar cycle. In the descending half the vernal density becomes higher than the autumnal density. The periodograms obtained from a Fourier analysis of the daytime average density shows that the annual variation is dominant over the semiannual variations for low to moderate solar activity whereas the semiannual peak becomes dominant over annual peak for high solar activity irrespective of the latitudes. At night, however, latitudinal differences have been observed. The annual variation is stronger than the semiannual variation at 10° N for low to moderate solar activity while for high solar activity the situation reverses. At 10° S and the magnetic equator, the annual variation is dominant for all levels of solar activity. Amplitude of the annual variation is higher in winter compared to that in summer. The physical and dynamical processes responsible for the observed annual and semiannual trends in topside density will be identified and discussed.

Keywords: Electron density, F-region, equatorial ionosphere, annual and semiannual variation.

1. INTRODUCTION

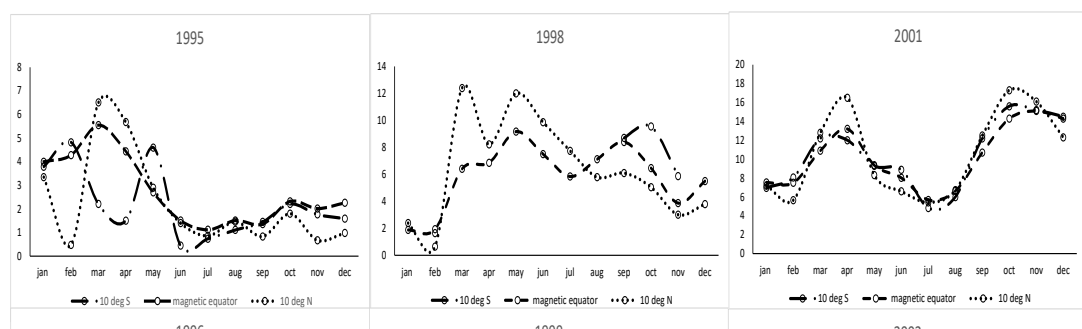
Ionospheric parameters such as peak electron density of the ionospheric F2 layer (NmF2), the height of the F2-layer peak (hmF2), electron density, electron temperature exhibits annual and semiannual variations. Rishbeth et al. 1999, used ionosonde data from sixteen stations to make an extensive study on annual and semiannual variations in hmF2

over mid latitudes. Zou et al. 2000 used ionosonde data to study annual, seasonal and semiannual variations of NmF2 and hmF2 over Slough (52° N, 1° W), Kerguelen (49° S, 70° E), Wallops Island (38° N, 75° W), Hobart (43° S, 147° E), Wakkanai (38° N, 142° E), Port Stanley (52° S, 58° W) and compared with the coupled thermosphere-ionosphere-plasmasphere computational model (CTIP) for geomagnetically quiet conditions. Su et al. 1998 observed annual and seasonal variations in the low-latitude topside electron density using observations made by the Hinotori satellite and the Sheffield University Plasmasphere Ionosphere Model (SUPIM).

The annual and semiannual variation of ionospheric parameters has been extensively studied in various parts of world. In this paper we present the yearly variation of electron density at 500 km/600 km altitudes over $\pm 10^\circ$ magnetic and the magnetic equator of the Indian subcontinent for the solar cycle 23.

2. Method

For this analysis we have used the electron density Ne data as measured by the Retarding Potential analyzer (RPA) on board SROSS C2 and ROCSAT-1 for the period 1995-2000 and 2001-2003 respectively. Observations (Fig. 1) reveal the existence of an equinoctial asymmetry during daytime (10:00-14:00 hrs) with higher electron density in spring than in autumn for both ascending and over descending leg of the solar cycle. The percentage increase of Ne in equinoxes over that in summer are given in Table I. The percentages have been derived after solar activity normalization



of observed electron density for each year. As shown in Table I the percentage increase of Ne in spring is higher than that in autumn over all the three latitudes. The rate of increase of Ne in spring slows with increasing solar activity. Further the difference between the levels of electron density in the two equinoxes decreases with increasing solar activity irrespective of latitude.

At night (22:00-00:00 hrs), electron density is higher in autumn than that in Spring during low solar activity whereas for moderate and high solar activity electron density becomes higher in spring than in autumn in all the three latitudes (Fig. 2). The percentage increase of electron density in the equinoxes over that in summer are shown in Table II.

Results and discussion

2.1 Fourier analysis

Fig. 3 – 8 shows periodograms obtained from Fourier analysis for the $\pm 10^\circ$ magnetic equator and over the magnetic equator from 1995 to 2003 and for both daytime and nighttime. The periodograms show that during daytime the annual variation is dominant over the semiannual variation for the ascending half of the solar cycle while for the descending leg semiannual peak becomes stronger than the annual peak over all the three latitudes. Fig. 6 shows that over 10° N magnetic latitude nighttime annual variation is dominant for the ascending leg and semiannual variation is dominant for the descending leg of the solar cycle. But over the magnetic equator and over 10° S magnetic, the annual peak is dominant over the semiannual peak for all levels of solar activity. Due to unavailability of data some years are missing over 10° S of the magnetic equator.

Table I: Percentage of increase of daytime electron density in equinoxes over the values in summer

Year	10o S magnetic		0o magnetic		10o N magnetic	
	spring	autumn	spring	autumn	spring	autumn
1995	94	34	83	5	137	-42
1996	121	43	100	4	178	-62
1997	80	29	73	5	117	-31
1998	35	14	33	7	51	2
1999	25	10	22	8	36	10
2000	21	9	17	8	29	13
2001	20	9	16	8	29	13
2002	21	9	17	8	30	13
2003	31	12	28	7	45	5

Ne x (10¹⁰ m⁻³)

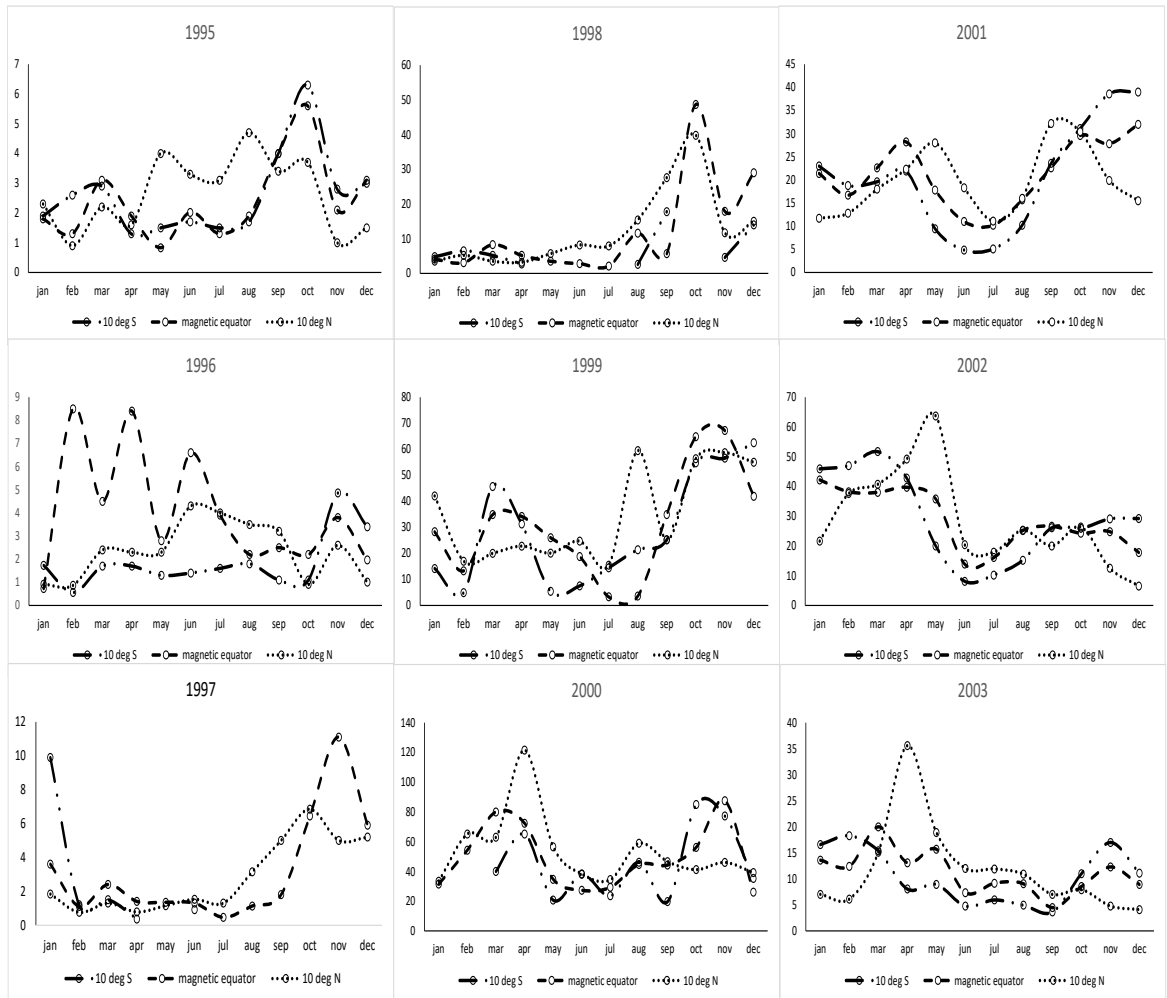


Fig 2

Table II: Percentage of increase of nighttime electron density in equinoxes over the values in summer

Year	10° S magnetic		0° magnetic		10° N magnetic	
	spring	autumn	spring	autumn	spring	autumn
1995	12	173	16	59	5	76
1996	-31	239	-46	97	-40	160
1997	30	146	32	49	16	56
1998	75	78	58	33	34	24
1999	83	65	61	31	36	20
2000	87	60	63	30	37	18
2001	87	60	63	30	37	18
2002	86	61	63	30	37	18
2003	79	72	59	32	25	22

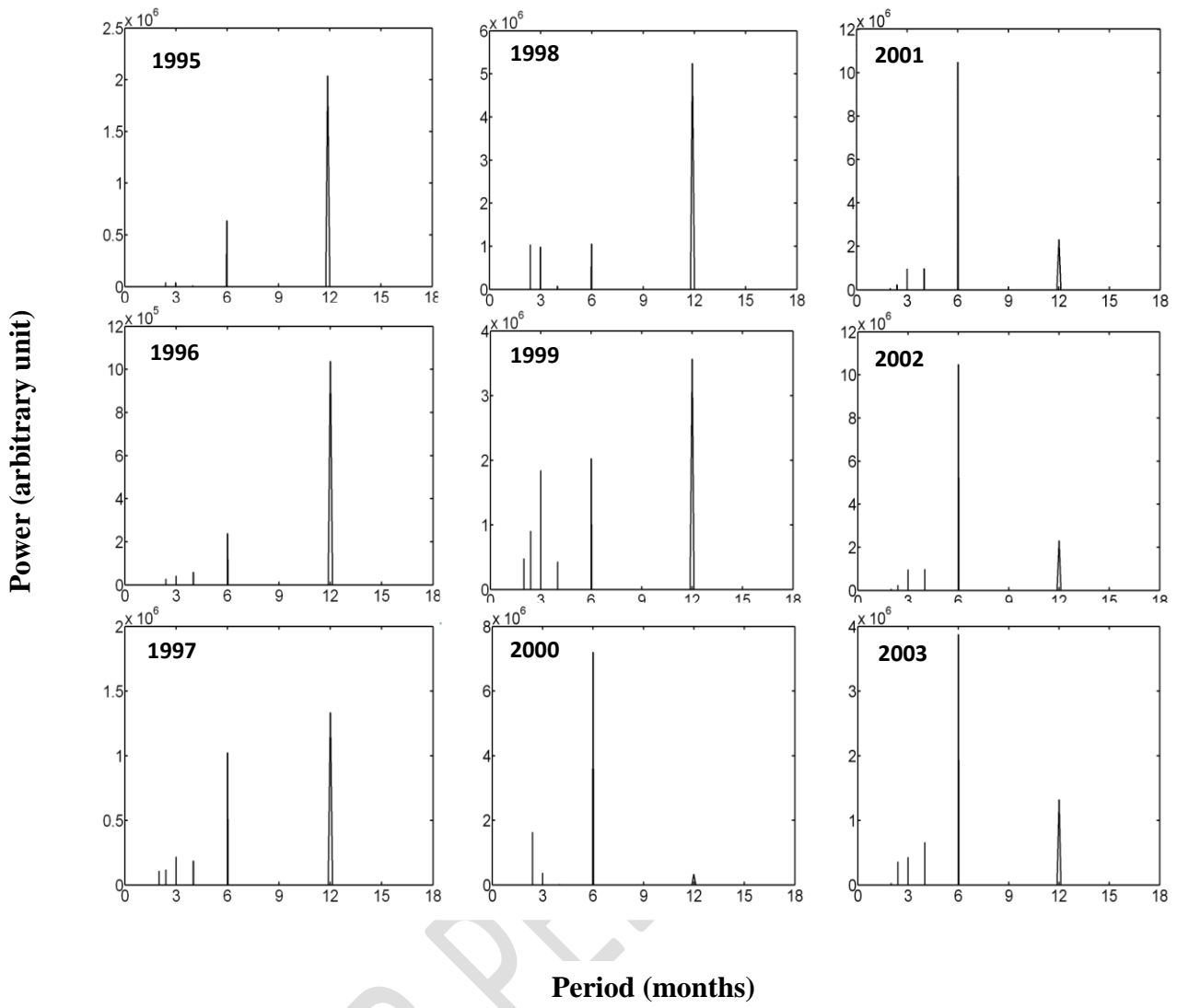


Fig. 3.

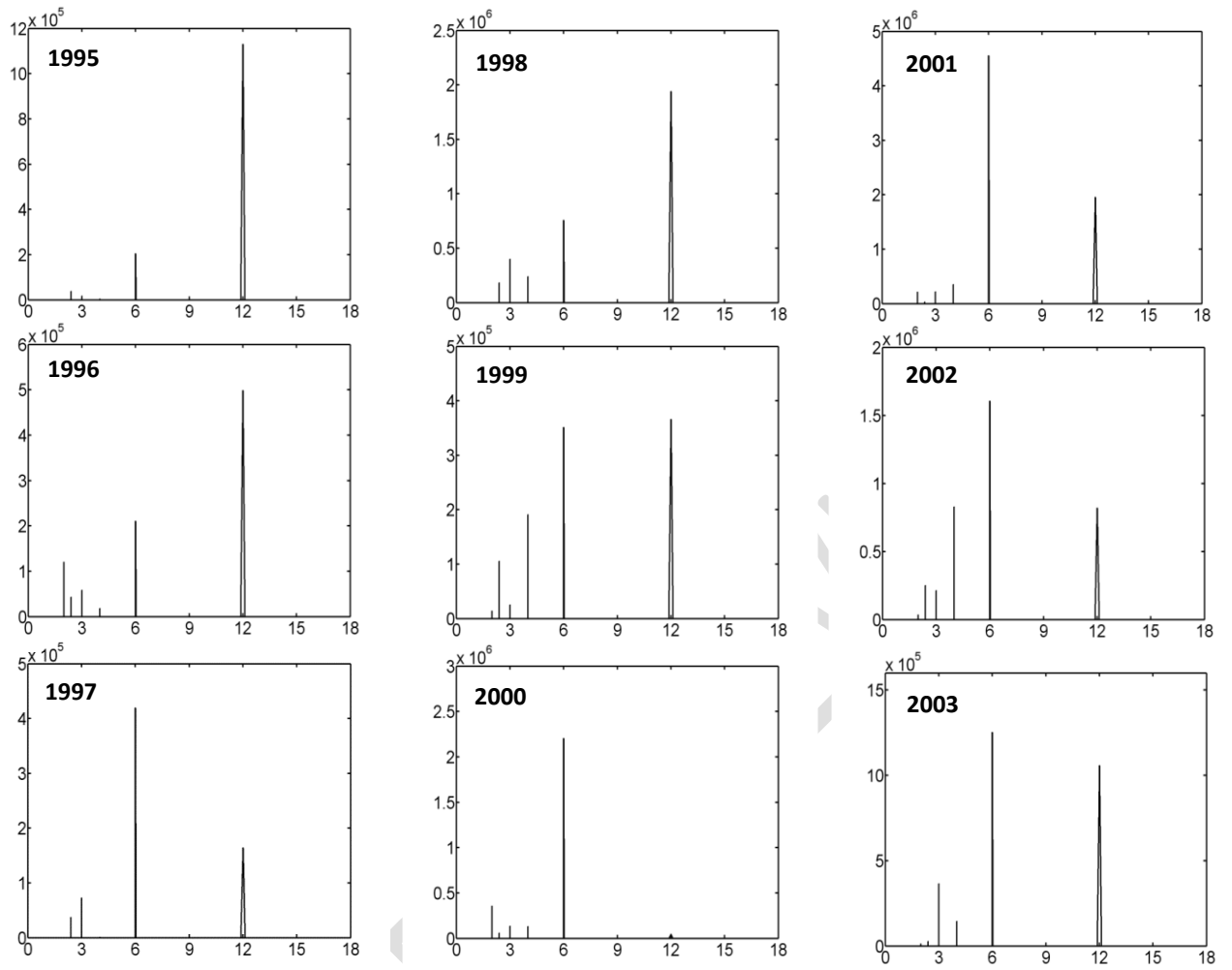


Fig. 4

Power (arbitrary unit)

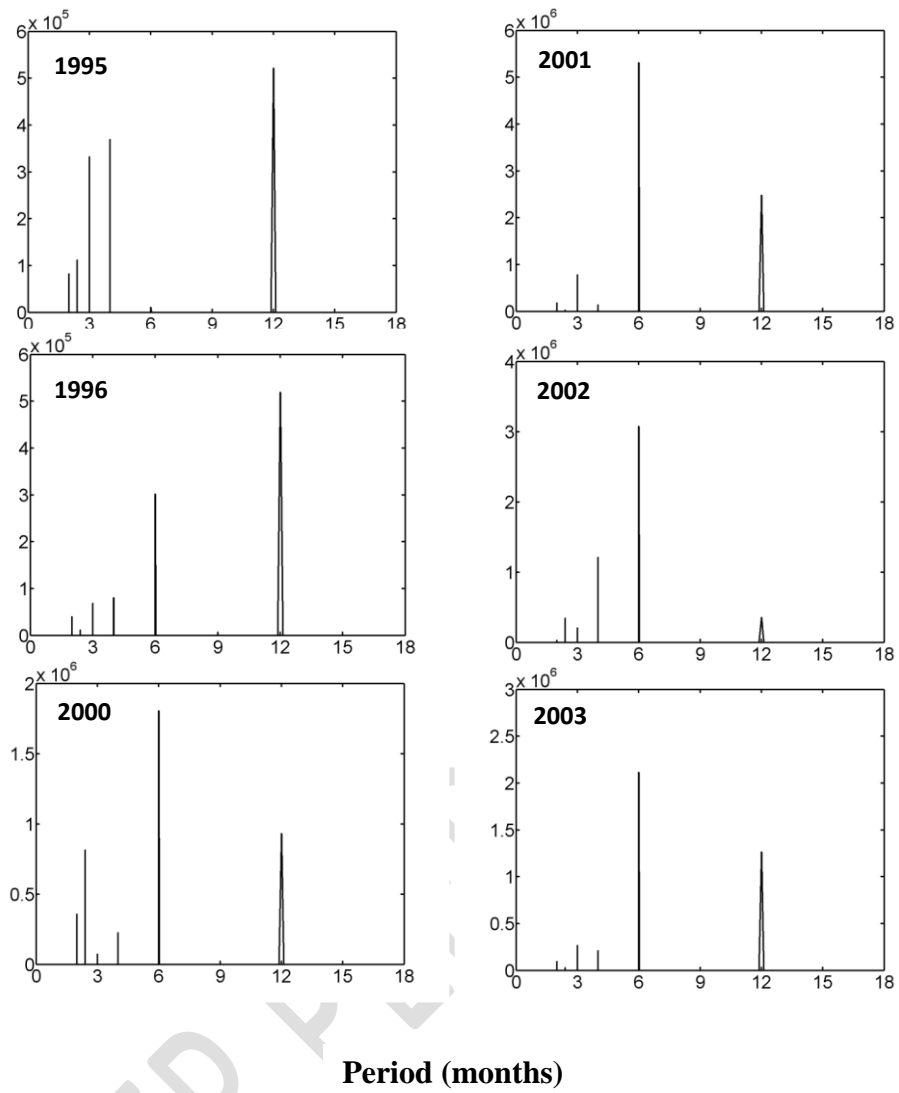


Fig. 5

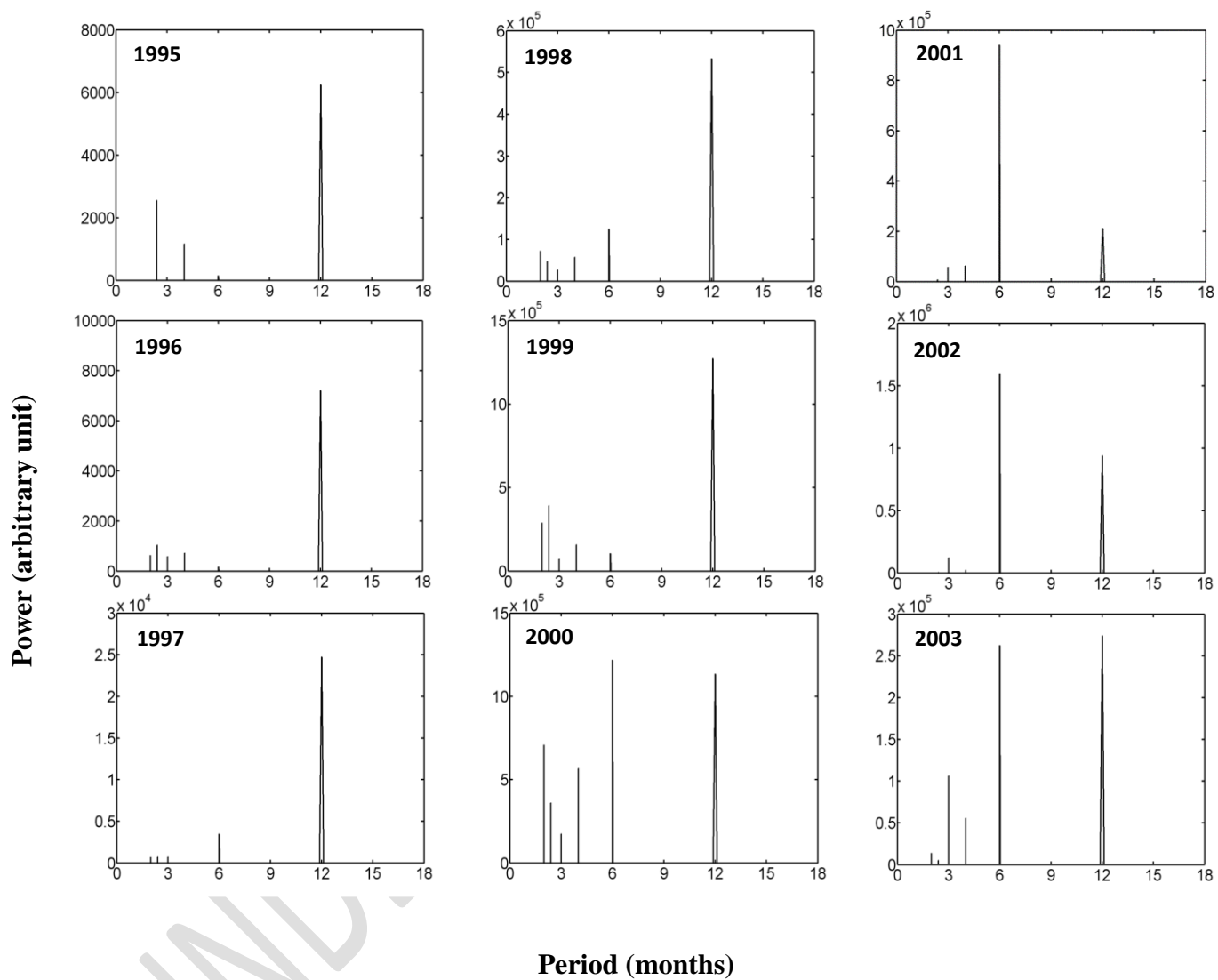


Fig. 6

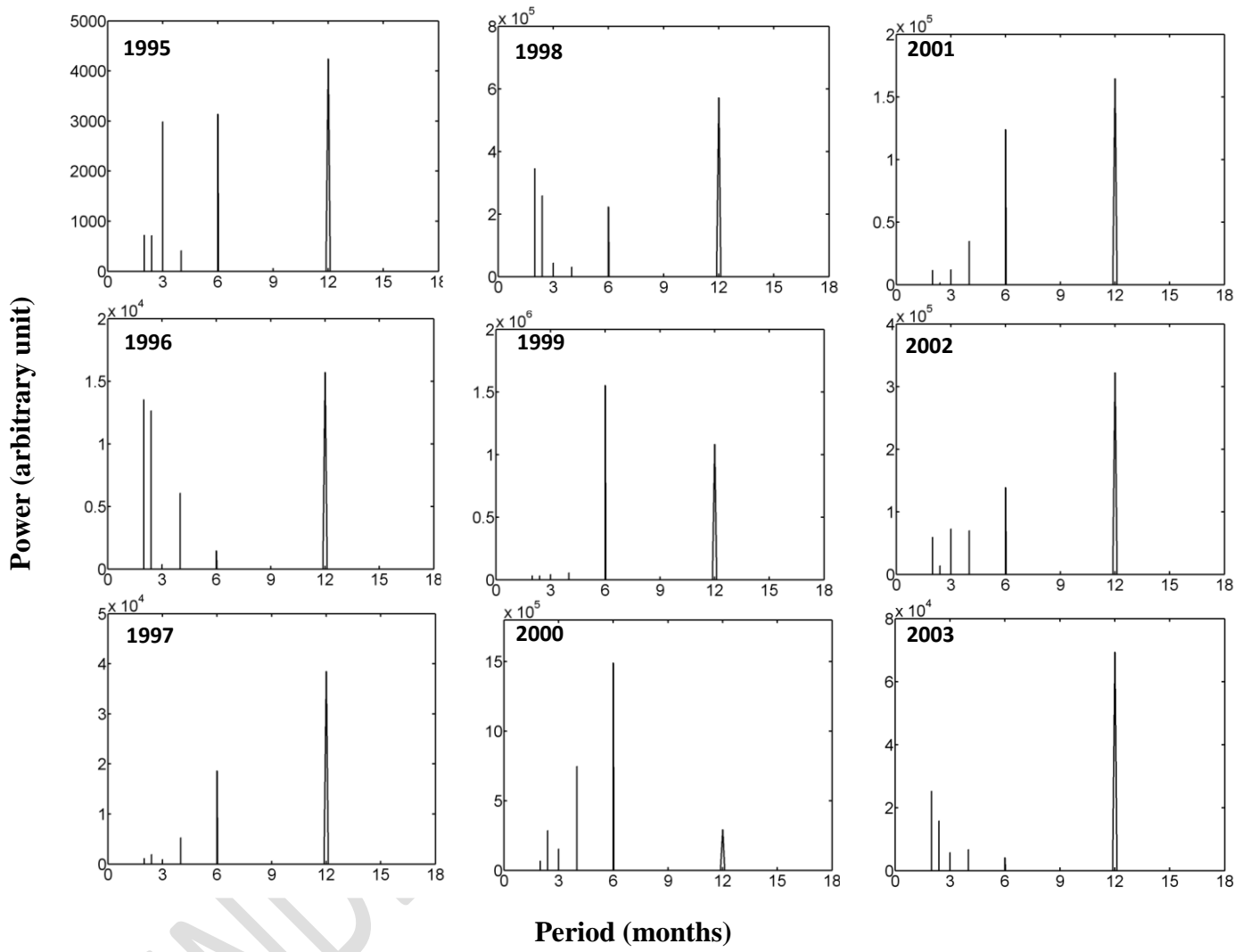


Fig. 7

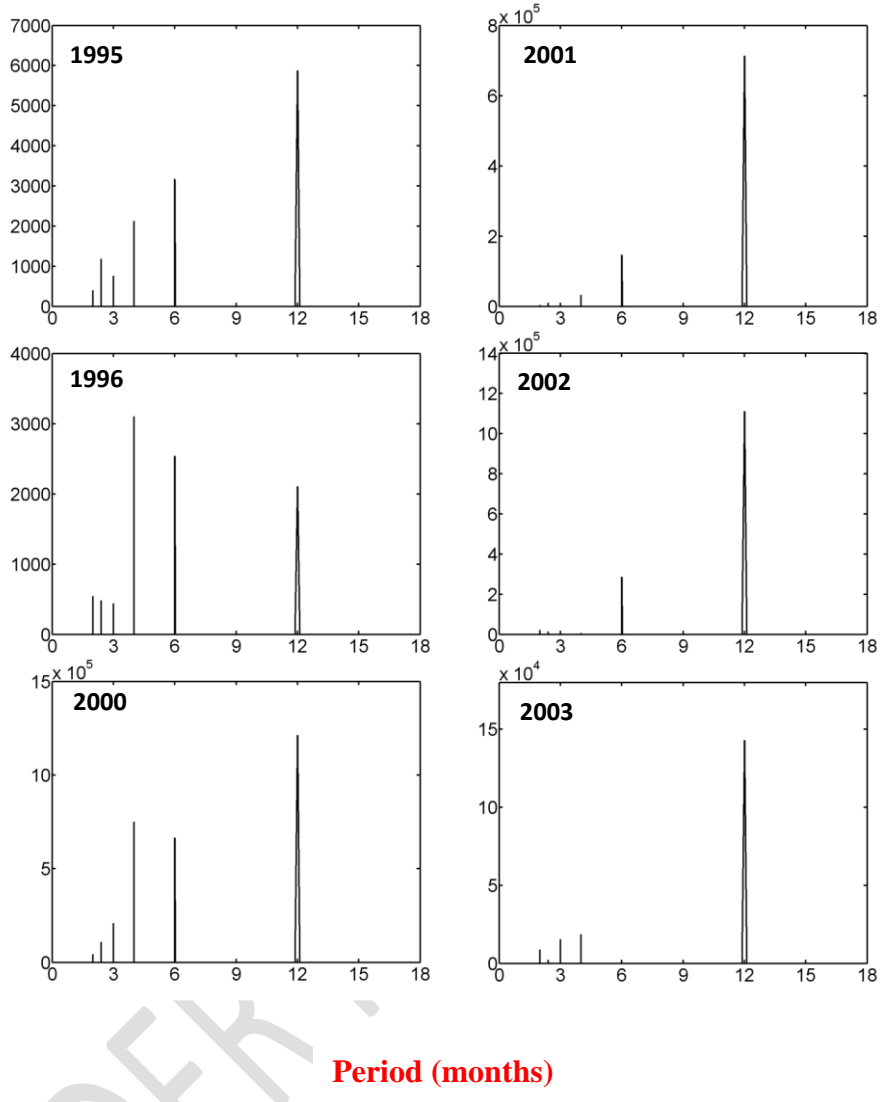


Fig. 8

2.1.1 Annual and semiannual components

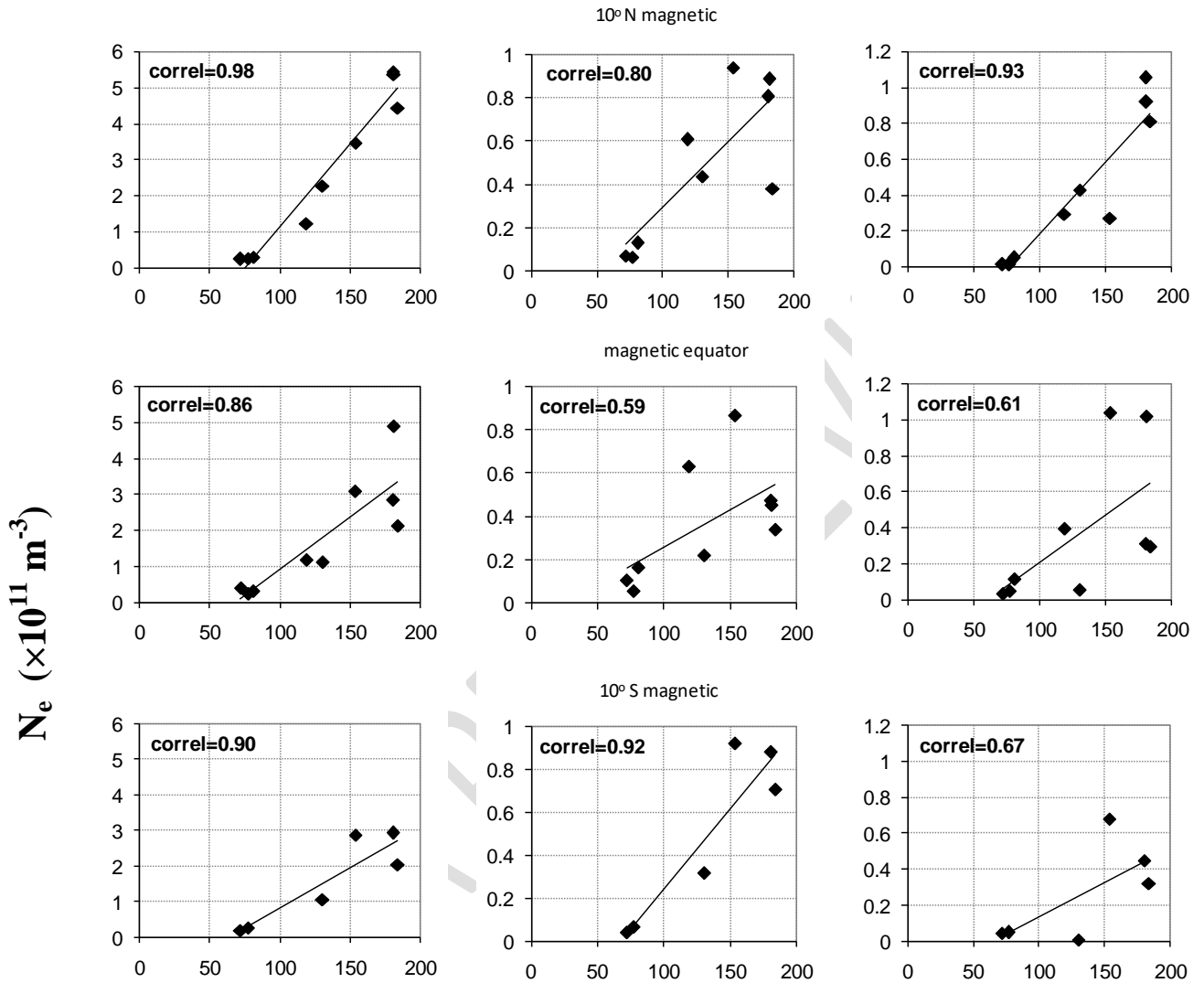
Fig. 9 shows amplitudes of the mean (a_0), annual (a_1) and semiannual (a_2) components of Ne obtained from Fourier analysis plotted against the annual mean values of F10.7 over the three latitudes for daytime. A regression analysis indicates very good correlation of the annual means (~ 0.96 - ~ 0.98) and semiannual (~ 0.81 - ~ 0.91) amplitudes with F10.7 cm solar flux. The annual component has poor correlation with F10.7 over all the three latitudes. Fig. 10 shows variation of nighttime amplitude a_0 , a_1 and a_2 of Ne over $\pm 10^\circ$ magnetic and over the magnetic equator. The semiannual amplitude has better correlation with F10.7 over 10° N magnetic than over the magnetic equator and over 10° S of the magnetic equator. The nighttime annual amplitude has good correlation (~ 0.59 - ~ 0.92) with F10.7 over all the three latitudes.

As for phases, taking 1st January as 0 phase Tables III- V shows that while the annual phase fluctuates between summer and winter for both daytime and nighttime over all the three latitudes the semiannual variation is consistently near equinoxes irrespective of year and latitude.

2.3 Semiannual variation and MSIS model

The global distribution of daytime electron density at the F2 layer is essentially determined by the sun, and by the chemical composition of the neutral air upon which the sun's radiation acts. The important chemical parameter is the atomic/molecular ratios in the F2 layer, conveniently specified by the O/N₂ concentration ratio.

To determine the O/N₂ ratio at 500 km altitude we ran the Mass Spectrometer and Incoherent Scatter radar-2000 (MSIS-2000) model (J. M. Picone et al. 2002) for the $\pm 10^\circ$ magnetic and over the geomagnetic equator for each month of the corresponding years at the local time 12:00 LT and for $A_p = 15$ to represent average condition and for annual



F10.7 flux

Fig 10

Table III : Annual mean, annual and semiannual amplitude and phases over 10° N magnetic

	Year	Annual mean (a_0) ($\times 10^{11} \text{ m}^{-3}$)	Amplitude		Phases	
			a_1 ($\times 10^{11}$ m^{-3})	a_2 ($\times 10^{11}$ m^{-3})	Φ_1 (radians)	Φ_2 (radians)
DAY	1995	2.56	1.19	0.66	5.21	4.11
	1996	1.77	0.85	0.41	4.76	3.35
	1997	2.71	0.96	0.84	4.63	3.3
	1998	6.07	1.91	0.86	4	2.82
	1999	11.63	1.57	1.19	3.83	2.89
	2000	17.62	0.48	2.24	3.11	3.22
	2001	17.19	1.27	2.70	0.70	3.05
	2002	19.11	1.01	2.03	5.57	4.34
	2003	10.95	0.96	1.64	5.59	3.5
NIGHT	1995	0.26	0.07	0.01	2.94	4.71
	1996	0.24	0.07	0.01	3.23	0.16
	1997	0.28	0.13	0.05	1.46	2.74
	1998	1.22	0.61	0.29	1.8	3.41
	1999	3.48	0.94	0.27	1.28	1.74
	2000	5.37	0.89	0.92	4.79	3.57
	2001	4.43	0.38	0.81	3.03	3.40
	2002	5.45	0.81	1.05	4.39	3.72
	2003	2.27	0.44	0.43	4.54	3.33

Table IV: Annual mean, annual and semiannual amplitude and phases over 0° magnetic

	Year	Annual mean (a_0) ($\times 10^{11} \text{ m}^{-3}$)	Amplitude		Phases	
			a_1 ($\times 10^{11}$ m^{-3})	a_2 ($\times 10^{11}$ m^{-3})	Φ_1 (radians)	Φ_2 (radians)
DAY	1995	2.76	0.81	0.38	5.52	4.08
	1996	2.50	0.59	0.38	4.86	3.70
	1997	2.70	0.34	0.54	4.69	3.45
	1998	5.90	1.16	0.73	3.26	2.92
	1999	11.36	0.50	0.49	2.89	2.68
	2000	13.11	0.18	1.24	5.85	3.00
	2001	10.27	1.17	1.78	0.66	2.68
	2002	11.50	0.76	1.06	6.22	4.13
	2003	6.79	0.86	0.93	5.32	3.88
NIGHT	1995	0.24	0.05	0.05	1.4	3.49
	1996	0.40	0.10	0.03	4.69	3.75
	1997	0.32	0.16	0.11	0.89	2.14
	1998	1.18	0.63	0.39	1.22	2.68
	1999	3.09	0.87	1.04	0.78	2.66
	2000	4.90	0.45	1.02	6.15	3.48
	2001	2.13	0.34	0.29	0.52	2.87
	2002	2.86	0.47	0.31	5.51	4.12
	2003	1.12	0.22	0.05	5.30	3.37

Table V: Annual mean, annual and semiannual amplitude and phases over 10° S magnetic

	Year	Annual mean (a_0) ($\times 10^{11} \text{ m}^{-3}$)	Amplitude		Phases	
			a_1 ($\times 10^{11}$ m^{-3})	a_2 ($\times 10^{11}$ m^{-3})	Φ_1 (radians)	Φ_2 (radians)
DAY	1995	2.19	0.60	0.09	5.74	4.51
	1996	2.49	0.60	0.46	5.24	3.45
	1997					
	1998					
	1999					
	2000	14.65	0.80	1.12	4.54	3.49
	2001	10.47	1.31	1.92	0.73	2.78
	2002	12.53	0.50	1.46	5.87	4.08
	2003	7.60	0.94	1.21	5.75	3.68
NIGHT	1995	0.26	0.06	0.05	1.25	3.48
	1996	0.19	0.04	0.04	0.90	1.64
	1997					
	1998					
	1999	2.87	0.92	0.68	0.89	2.76
	2000					
	2001	2.04	0.70	0.32	0.64	2.68
	2002	2.93	0.88	0.45	5.93	4.19
	2003	1.05	0.32	0.01	6.18	5.67

mean values of F10.7: 77, 72, 81, 119, 153, 181, 184, 180, 130 for the years 1995, 1996, 1997, 1998, 1999, 2000, 2001, 2002 and 2003 respectively. Table VI shows the percentage

increase of O/N_2 ratio at noon in spring and autumn over that in summer as derived from the MSIS-2000 model. The O/N_2 ratio in spring is higher than the autumn over 10° S magnetic and over 10° N magnetic, where autumnal O/N_2 ratio is slightly higher than the vernal O/N_2 ratio irrespective of solar activity.

Table VII shows the percentage increase of O/N_2 ratio in equinoxes above the value in summer at midnight (0:00 LT) over $\pm 10^\circ$ magnetic and over the magnetic equator derived from MSIS-2000 model. The model is in agreement with observations over 10° S magnetic and over magnetic equator for moderate and high solar activity and over 10° N magnetic for low solar activity.

2.4 CONCLUSION

Yearly variations of the F-region electron density in the Indian zone have been investigated using SROSS C2 and FORMOSAT – 1 data. The observations show the existence of an equinoctial asymmetry over India with higher values of electron density in spring than in autumn during daytime. At night electron density in autumn becomes higher than in spring for low solar activity while for moderate and high solar activity N_e in spring is higher than that in autumn. Daytime annual and semiannual variation has no latitudinal variation while nighttime annual and semiannual variation shows latitudinal variation. We find that annual and semiannual variation has well-defined relationship with solar activity. The semiannual variation has almost constant phase near equinox and its amplitude increases with increasing F10.7 both during daytime and nighttime over all the three latitudes. Daytime annual variation is unaffected by

Table VI: Percentage of increase of O/N2 ratio derived from MSIS-2000 model at noon in the equinoxes over those in summer

Year	10° S magnetic		0° magnetic		10° N magnetic	
	spring	autumn	spring	autumn	spring	autumn
1995	-3	-7	2	0.3	7	9
1996	-4	-8	1	-1	6	7
1997	-2	-7	3	1	8	10
1998	3	-2	10	8	17	18
1999	5	1	13	11	20	22
2000	7	2	15	13	23	25
2001	7	2	15	13	23	25
2002	7	2	15	13	23	24
2003	4	-1	11	9	18	20

Table VII: Percentage of increase of O/N2 ratio derived from MSIS-2000 model at night (00:00 hr) in the equinoxes over those in summer

Year	10° S magnetic		0° magnetic		10° N magnetic	
	spring	autumn	spring	autumn	spring	autumn
1995	-3	-7	2	0.3	7	9
1996	-4	-8	1	-1	5	7
1997	-2	-7	3	1	20	22
1998	3	-2	10	8	16	18
1999	5	0.5	13	11	20	22
2000	7	2	15	13	23	25
2001	7	2	15	13	23	25
2002	7	2	15	13	23	24
2003	4	-1	11	9	18	20

solar activity with very poor correlation of its amplitude with F10.7. But at night the amplitude of the annual variation of electron density increases with increasing F10.7.

The annual and semiannual variations in electron density of the F region have been considered to be due to one or more of the following mechanisms:

1. Composition changes due to global thermospheric circulation – the mechanism studied by Millward et al. (1996) and Rishbeth et al. (2000).
2. Variations in geomagnetic activity.
3. Solar wind energy (Lal. 1992, 1998).
4. Inputs from below, due to atmospheric waves and tides.
5. Changes in atmospheric turbulence.
6. Anisotropy of solar EUV emission in solar latitude (Burkard, 1951).

As suggested by Fuller-Rowell (1998) the semiannual anomaly is caused by the “thermospheric spoon”, i.e., the global thermospheric circulation at solstices raises the molecular nitrogen and oxygen densities and therefore reduces the atomic oxygen density compared with the equinoxes. Because N_2 and O control the loss rate and production rate of the plasma respectively, a low O/N_2 ratio gives rise to low electron densities in the ionosphere. The O/N_2 ratio depends on motions and chemical changes driven by solar radiation absorbed within the thermosphere.

No one to one correlation has been found between the electron density and geomagnetic activity over the Indian zone. The MSIS-2000 model simulations produce a reasonably good representation of the annual and semiannual variations of Ne for low geomagnetic activity condition.

Lal (1992, 1998) regards the “solar wind” as the cause of all semiannual aeronomic phenomena. The solar wind is on the other hand connected to the geomagnetic activity. For example, according to the theory of Russell and McPherron (1973), the semiannual variation of geomagnetic activity depends on the varying geometrical coupling of the interplanetary and terrestrial magnetic fields.

Zou et al. (2000) have studied about how waves and tides in the underlying mesosphere may affect the F2 layer, but they concluded that they are unlikely to have a major effect on annual and semiannual variations of $NmF2$.

Regarding the mechanism of changes in atmospheric turbulence, Shimazaki (1972) showed that large-scale convection motions have much more effect on thermospheric composition than changes in eddy diffusion at the turbopause, even though the “spoon” terminology might be thought to imply increased turbulent mixing.

The hypothesis that the Sun’s EUV radiation varies with heliographic latitude (Burkard, 1951), combined with the semiannual variation of the Earth’s heliographic latitude, is dismissed due to lack of evidence to support it.

REFERENCES

1. Rishbeth H., and Muller-Wodarg I. C. F., Vertical circulation and thermospheric composition: a modelling study. *Ann. Geophysicae*. 1999; 17: 794-805.
2. Zou L., Rishbeth H., Muller-Wodarg I. C. F., Aylward A. D., Millward G. H., Fuller-Rowell T. J., Idenden D. W., Moffett R. J., Annual and semiannual variations in the ionospheric F2-layer. I. Modelling. *Ann. Geophysicae*. 2000; 18, 927-944.
3. Su Y. Z., Bailey G. J., Oyama K. I., Annual and seasonal variations in the low-latitude topside ionosphere. *Ann. Geophysicae*. 1998; 16, 974-985.
4. Picone J. M., Hedin A. E., Drob D. P., Aikin A. C., NRLMSISE-00 empirical model of the atmosphere: statistical comparison and scientific issues. *J. Geophys. Res.* 2002; 107(A12), 1468.
5. Millward G. H., Rishbeth H., Moffett R. J., Quegan S., Fuller-Rowell T. J., Ionospheric F2 layer seasonal and semiannual variations. *J. Geophys. Res.* 1996; 101, 5149-5156.
6. Rishbeth H., Muller-Wodarg I. C. F., Zou L., Fuller-Rowell T. J., Millward G. H., Moffett R. J., Idenden D. W., Aylward A. D., Annual and semiannual variations in the ionospheric F2-layer: II. Physical discussion. *Ann. Geophysicae*. 2000; 18, 945-946.
7. Lal, Chaman, Global F2 layer ionization and geomagnetic activity. *J. Geophys. Res.* 1992; 97, 12 153-12 159.

8. Lal, Chaman, Solar wind and equinoctial maxima in geophysical phenomena. J. Atmos. Terr. Phys.. 1998; 60, 1017-1024.
9. Burkard O., Die halbjährige Periode der F2-Schicht-Ionisation. Archiv. Meteorol. Biokim. Wien. 1951; 4, 391-402.
10. Fuller-Rowell T. J., The thermospheric spoon" a mechanism for the semi-annual density variation. J. Geophys. Res.. 1998; 103, 3951-3956.
11. Russel C. T., McPherron R. L., Semiannual variation of geomagnetic activity. J. Geophys. Res.. 1973; 78, 92-107.
12. Shimazaki T., Effects of vertical mass motions on the composition structure in the thermosphere. Space Research. 1972; 12, 1039-1045.

FIGURE CAPTIONS

Fig. 1 Yearly variation of electron density during daytime at 500 km altitude.

Fig. 2 Yearly variation of electron density during nighttime at 500 km altitude.

Fig. 3 Periodogram of electron density during daytime over 10° N magnetic.

Fig. 4 Periodogram of electron density during daytime over 0° magnetic.

Fig. 5 Periodogram of electron density during daytime over 10° S magnetic.

Fig. 6 Periodogram of electron density during nighttime over 10° N magnetic.

Fig. 7 Periodogram of electron density during nighttime over 0° magnetic.

Fig. 8 Periodogram of electron density during nighttime over 10° S magnetic.

Fig. 9 Amplitude of mean, annual and semiannual components of Ne (from left to right) plotted against 10.7 cm solar flux at three latitudes for day time (10:00-14:00 LT).

Fig. 10 Amplitude of mean, annual and semiannual components of Ne (from left to right) plotted against 10.7 cm solar flux at three latitudes for night time (22:00-00:00 LT).